

Accepted Article Preview: Published ahead of advance online publication



Distinct Impact of two Keratin Mutations Causing Epidermolysis Bullosa Simplex on Keratinocyte Adhesion and Stiffness

Melanie Homberg, Lena Ramms, Nicole Schwarz, Georg Dreissen, Rudolf E Leube, Rudolf Merkel, Bernd Hoffmann, Thomas M Magin

Cite this article as: Melanie Homberg, Lena Ramms, Nicole Schwarz, Georg Dreissen, Rudolf E Leube, Rudolf Merkel, Bernd Hoffmann, Thomas M Magin, Distinct Impact of two Keratin Mutations Causing Epidermolysis Bullosa Simplex on Keratinocyte Adhesion and Stiffness, *Journal of Investigative Dermatology* accepted article preview 11 May 2015; doi: [10.1038/jid.2015.184](https://doi.org/10.1038/jid.2015.184).

This is a PDF file of an unedited peer-reviewed manuscript that has been accepted for publication. NPG are providing this early version of the manuscript as a service to our customers. The manuscript will undergo copyediting, typesetting and a proof review before it is published in its final form. Please note that during the production process errors may be discovered which could affect the content, and all legal disclaimers apply.

Received 26 February 2015; revised 10 April 2015; accepted 25 April 2015;
Accepted article preview online 11 May 2015

Distinct impact of two keratin mutations causing epidermolysis bullosa simplex on keratinocyte adhesion and stiffness

Short title: Impact of K14R131P on cell adhesion and stiffness

Melanie Homberg^a, Lena Ramms^b, Nicole Schwarz^c, Georg Dreissen^b, Rudolf E. Leube^c, Rudolf Merkel^b, Bernd Hoffmann^b, Thomas M. Magin^{a,2}

^aInstitute of Biology and Translational Center for Regenerative Medicine, University of Leipzig, 04103 Leipzig, Germany

^bInstitute of Complex Systems, ICS-7: Biomechanics, Forschungszentrum Jülich, 52425 Jülich, Germany

^cInstitute of Molecular and Cellular Anatomy, RWTH Aachen University, 52074 Aachen, Germany

²Corresponding Author:

Thomas M. Magin, Translational Center for Regenerative Medicine (TRM) and Institute of Biology, Cell and Developmental Biology, University of Leipzig, Philipp-Rosenthal-Straße 55, D-04103 Leipzig, Germany, phone 0049(0)341 97 39582, fax 0049(0)341 97 39589, thomas.magin@trm.uni-leipzig.de

Abbreviations

AFM – Atomic force microscopy

DP – Desmoplakin

EBS – Epidermolysis bullosa simplex

K – Keratin

KIF – Keratin intermediate filament

KtyI – Keratin type I gene cluster

KtyII – Keratin type II gene cluster

WB – Western Blot

WT - Wildtype

Accepted manuscript

ABSTRACT

Keratin filaments constitute the major component of the epidermal cytoskeleton from heterodimers of type I and type II keratin subunits. Missense mutations in K5 or K14, highly expressed in the basal epidermis, cause the severe skin blistering disease epidermolysis bullosa simplex in human by rendering the keratin cytoskeleton sensitive to mechanical stress, yet the mechanisms by which individual mutations cause cell fragility are incompletely understood.

Here, we compared the K14p.Arg131Pro to the K5p.Glu471Asp mutation, both giving rise to severe generalized EBS, by stable expression in keratin-free keratinocytes. This revealed distinctly different effects on keratin cytoskeletal organization, in agreement with *in vivo* observations, thus validating the cell system. While the K14p.Arg131Pro mutation led to impaired desmosomes, downregulation of desmosomal proteins and weakened epithelial sheet integrity upon shear stress, the K5p.Glu471Asp mutation did not impair these functions although causing EBS with squamous cell carcinoma *in vivo*. Atomic force microscopy demonstrated that K14R131P cells were even less resistant against deformation than keratin-free keratinocytes. Thus, a keratin mutation causing EBS compromises cell stiffness to a greater extent than the lack of keratins. Finally, re-expression of K14 in K14R131P cells did not rescue the above defects. Collectively, our findings have implications for EBS therapy approaches.

INTRODUCTION

The skin protects the body against pathogens, dehydration and diverse mechanical stresses (Simpson *et al.*, 2011). Mutations in K5 or K14 which form the major cytoskeleton in basal keratinocytes cause epidermolysis bullosa simplex (EBS), characterized by loss of tissue integrity and severe blistering of the skin upon mild mechanical trauma (Coulombe and Lee, 2012; Fuchs and Weber, 1994; Homberg and Magin, 2014). K14p.Arg125, located in the helix initiation motif of K14, is the most frequently mutated residue and gives rise to severe generalized EBS (formerly known as EBS Dowling-Meara) (Fine *et al.*, 2014) with extensive cytoplasmic keratin aggregates (www.interfil.org) (Szeverenyi *et al.*, 2008). The K5p.Glu477Asp mutation in the helix termination motif of K5 causes severe generalized EBS accompanied by massive verrucous carcinoma (Schumann *et al.*, 2012). The mechanisms by which these and additional mutations cause EBS and contribute to the very rare occurrence of basal cell or squamous cell carcinoma (Baek *et al.*, 2011; Schumann *et al.*, 2012; Stacey *et al.*, 2009) remain incompletely understood.

In EBS keratinocytes, downregulation of cell junction components (Liovic *et al.*, 2009) and impaired resilience to mechanical stress (Russell *et al.*, 2004) was reported. Adding to the complexity of pathomechanisms causing EBS (for altered cytokine signaling see (Roth *et al.*, 2012b)), desmosome maintenance was shown to depend on stable interactions with keratins. Absence of keratins caused a PKC α -mediated hyperphosphorylation of desmoplakin and compromised epithelial adhesion (Bar *et al.*, 2014; Kroger *et al.*, 2013).

Moreover, keratins represent major determinants of cell stiffness, as shown by using either optical stretcher (Seltmann *et al.*, 2013a) or atomic force microscopy (AFM) (Ramms *et al.*, 2013). Remarkably, re-expression of substoichiometric amounts of K5/K14 rescued intercellular adhesion defects and normalized cell stiffness. Given that keratinocyte adhesion and resilience against mechanical force are compromised in EBS, this raises the question whether distinct keratin mutations act in a similar way. To address this, we generated stable mouse keratinocyte cell lines expressing K14p.Arg131Pro (corresponding to the human K14p.Arg125 residue) and K5p.Glu471Asp

(corresponding to the human K5p.Glu477 residue) in keratin-deficient keratinocytes lacking either the entire type I (KtyI^{-/-}) (Ramms *et al.*, 2013) or type II (KtyII^{-/-}) (Kroger *et al.*, 2013); Kumar *et al.*, unpublished) keratin cluster, respectively.

RESULTS & DISCUSSION

Two mutations causing severe generalized EBS display different impacts on cytoskeletal organization

To focus on mutation-specific effects, we compared the impact of K14p.Arg131Pro and K5p.Glu471Asp mutations upon stable expression in keratinocytes lacking all type I (KtyI^{-/-} K14R131P cells) or type II (KtyII^{-/-} K5E471D cells) keratin genes, respectively. Expression of WT-K14 (KtyI^{-/-} K14 cells) and WT-K5 (KtyII^{-/-} K5 cells) in appropriate keratin-deficient cells served as control to relate altered phenotypes directly to the keratin mutation.

As predicted, K14 formed a wildtype-like keratin cytoskeleton (Figure 1a). In contrast, K14R131P aggregates accumulated throughout the cytoplasm but failed to form any filaments, in contrast to *in vitro* settings (Figure 1a') (Herrmann *et al.*, 2002; Ma *et al.*, 2001). This was different from previous patient-derived or engineered cells co-expressing normal and mutant keratins, in which aggregates were mostly confined to the cell periphery and intact filaments surrounded the nucleus (Coulombe *et al.*, 1991a; Kitajima *et al.*, 1989; Morley *et al.*, 2003; Werner *et al.*, 2004). The latter might add to the notable resilience of keratinocytes expressing mutant keratins (Beriault *et al.*, 2012). The random size and distribution of keratin aggregates does not support a specific tethering mechanism (Figure S1a).

Unlike the strong, dominant-negative impact of K14R131P on keratin organization, microtubules and actin organization appeared unaltered in KtyI^{-/-} or K14R131P compared to WT and K14 controls (Figure S1b). To examine different amino acid substitutions reported for the K14p.Arg125 residue (www.interfil.org), K14p.Arg131Cys or K14p.Arg131His were expressed in KtyI^{-/-} cells, revealing

similar behavior as K14R131P (Figure S2a). Thus, in agreement with patient data, any of these mutations caused collapse into cytoplasmic keratin aggregates. Whether this results in similar functional consequences remains open and may be different for mutations generating a Cys residue that might be cross-linked upon oxidation (Lee *et al.*, 2012).

In contrast to K14R131P, K5E471D, which caused severe generalized EBS with verrucous carcinoma, formed an intact keratin cytoskeleton with endogenous K14, indistinguishable from the re-expression of K5 (Figure 1b,b'). To validate the aggregate-forming ability of this residue, K5p.Glu471Lys and K5p.Glu471Gly was transfected, both causing widespread aggregates, similar to K14p.Arg131Pro (Figure S2b). The occurrence of aggregates and filaments in non-lesional keratinocytes (Schumann *et al.*, 2012) suggests that K5E471D requires genetic modifiers to cause severe generalized EBS that should be traceable in our keratinocyte model.

Western blotting (WB) of protein lysates confirmed expression of WT-K14 and K14R131P (38-58%; Figure 1c) and of WT-K5 and K5E471D (17-28%; Figure 1d) in comparable ways. Of note, both wildtype and mutant K14 stabilized the endogenous binding partners K5 and K6 similarly (Figure 1c). This underscores the finding that in K14R131P cells, aggregates are positive for K5 and K6 (Figure S1a). Vice versa, expression of K5 or K5E471D stabilized K14 (Figure 1d).

Expression of K14R131P but not of K5E471D compromises desmosomal adhesion

The mutation-selective impact on cytoskeletal organization prompted the analysis of keratin-dependent desmosome distribution and adhesive strength (Bar *et al.*, 2014; Kroger *et al.*, 2013; Simpson *et al.*, 2011). Like in *KtyII^{-/-}* cells (Kroger *et al.*, 2013), desmoplakin (DP) which links keratins to the desmosomal cadherins via plakophilins and plakoglobin, was partially mislocalized throughout the cytoplasm, in addition to its membrane distribution, in *KtyI^{-/-}* cells (Figure S3a-a''). Re-expression of K5 or K14 in corresponding keratin-deficient cells shifted desmosomes to the plasma membrane in a wildtype-like manner (Figure 2a,b and Figure S3b-b''), while DP was mislocalized in K14R131P cells (Figure 2a'). Costaining for DP and K14 revealed a correlation between K14-positive aggregates and the amount of DP localized along cell membranes. Low numbers of K14R131P aggregates (L-cells

in Figure 2a') correlated with significant DP localization along cell borders, whereas cells expressing large numbers of aggregates (H-cells in Figure 2a') showed extensive cytoplasmic accumulation but almost no DP localized at cell-cell borders. Overall, DP mislocalization in K14R131P cells was worse than in *Ktyl*^{-/-} cells (Figure 2a' and Figure S3a-a''). To substantiate these data, images were quantified (for details see Figure S3c-c''). There was a decrease of ~12% for DP on cell-cell borders between two cells expressing high amount of aggregates (H-H Boundaries, Figure 2a'' and Figure S3c'') compared to cell-cell borders between two L-cells (L-L Boundaries; Figure 2a'' and Figure S3c''). By immunofluorescence analysis, no cytoplasmic co-localization of DP and aggregated keratins was found (Figure 2a'), contrasting previous reports (Russell *et al.*, 2004).

Unlike in K14R131P cells, DP distribution was unaltered in K5E471D cells. Thus, despite this mutation, the keratin cytoskeleton remained linked to desmosomes (Figure 2b'; compare with Figure S3b-b'').

The downregulation of DP shown for *Ktyl*^{-/-} keratinocytes (Kroger *et al.*, 2013), was also confirmed for *Ktyl*^{-/-} cells (~20% of WT level; Figure 3a,a'). Re-expression of wildtype K14 elevated DP amount to ~60% of WT level (Figure 3a,a'), while DP in K14R131P cells was reduced similar to *Ktyl*^{-/-} cells (Figure 3a,a'). Also, desmoglein (Dsg) 1 and 2 were reduced by 80% in K14R131P cells, whereas plakophilin-1 (PKP1) remained unchanged compared to controls (Figure S4a,b). In contrast to K14R131P transfectants, cells expressing K5E471D displayed levels of the above desmosomal proteins similar to K5 cells (Figure 3b,b' and Figure S4c,d). Downregulation of junctional proteins like DP, Dsg 3 and plakoglobin in heterozygous cells from EBS-patients was reported before (Liovic *et al.*, 2009), yet our data show that this reduction of desmosomal proteins is not common to all keratin mutations in EBS.

To address whether K14R131P-induced mislocalization of desmosomes affected intercellular adhesion, the sheet shear stress assay was performed (Hobbs *et al.*, 2011; Kroger *et al.*, 2013). As predicted, epithelial sheets fragmented in K14R131P mutants, in contrast to K14 cells (Figure 3c). At

the same time, the K5E471D mutation did not impact sheet integrity compared to K5 cells (Figure 3d).

This underlines that compromised desmosomal adhesion significantly contributes to EBS, in line with the occurrence of acantholysis in EBS-patients (Anton-Lamprecht and Schnyder, 1982; Darwich *et al.*, 2011). Moreover, DP or PKP1 mutations are associated with suprabasal EBS (Intong and Murrell, 2012). Further, EXPH5 mutations, affecting the Rab27B effector protein SlaC2-b involved in vesicle transport, cause an EBS-like disorder characterized by keratin collapse and disrupted desmosomes, supporting the hypothesis that pathomechanisms in EBS are more complex than previously thought (Liu *et al.*, 2014).

Expression of K14 in K14R131P cells fails to rescue epithelial sheet integrity

The ubiquitous presence of mutant keratins causing localized and recurrent blistering in the majority of EBS patients suggests that therapies resulting in localized repair might succeed. Based on a previous experiment (Bar *et al.*, 2014), K14R131P and WT cells were co-cultured at various ratios. This revealed that in presence of 70% WT cells, epithelial integrity in the shear stress assay was restored (Figure S5a). In cells grown at a 1:1 ratio, between WT cells KIF interconnected by desmosomes formed upon Ca^{2+} -mediated cell adhesion, while K14R131P cells failed to form cell-cell contacts (Figure 4a). Remarkably, “mixed” desmosomes between a WT and a K14R131P cell were also not properly established (Figure 4a,a’).

Given that the ratio of mutant and WT keratins determines IF or aggregate formation, we stably transfected HA tagged WT-K14 into K14R131P cells. Immunofluorescence analysis of cells grown in low Ca^{2+} revealed K14-positive IF in addition to aggregates, predominantly located in the cell periphery (Figure S5d), similar to heterozygous patient cells (Kitajima *et al.*, 1989; Morley *et al.*, 2003). Switching cells to high Ca^{2+} to induce junction formation revealed interconnected KIF between cells with fewer aggregates (L, Figure 4b); however, interaction of KIF to desmosomes was clearly disturbed in cells with many keratin aggregates (H, Figure 4b) and the mislocalization of DP persisted (Figure S5e). Furthermore, re-expression of K14HA in K14R131P cells failed to elevate DP

levels (Figure 4c and Figure S5f). Subjecting K14R131P cells re-expressing K14HA to the shear stress assay revealed that the presence of K14 was insufficient to rescue the strong phenotype of K14R131P cells (Figure 4d,d'). Although the overexpression of WT keratins as a therapeutic strategy for EBS has been supported by the finding that in mice transgenic for human K18p.Arg89Cys mutation, analogous to K14p.Arg125Cys, the ratio of mutant and WT keratins determines aggregate formation and affects embryo mortality (Cao *et al.*, 2001; Hesse *et al.*, 2007), more recent therapeutic strategies rather concentrate on the silencing of the mutant protein, for example with RNAi techniques (Hegde *et al.*, 2014; Roth *et al.*, 2012a).

Ktyl^{-/-} and K14R131P cells withstand cyclic stretch of intermediate amplitudes

In EBS, skin fragility occurs upon mild mechanical trauma. To investigate whether the K14R131P mutation resulted in impaired strain resilience, we performed cyclic stretch experiments on Ca²⁺-induced cell clusters. Two different stretch parameters were separately applied, using a single 40% strain and a cyclic 14% strain at 4 Hz for 90 min, respectively. For WT cells, 40% elongation caused no detectable rupture at cell-cell or cell-matrix adhesions (Figure S6). Identical strain resilience for all analyzed cell types was found in cyclic stretch experiments, accompanied by actin reorientation perpendicular to the strain direction, consistent with previous experiments (Figure 5) (Faust *et al.*, 2011).

Comparable results without measurable effects on intercellular adhesion were also found for Ktyl^{-/-} and K14R131P cells in single stretch experiments (Figure S6) and after cyclic stretch application (Figure 5). Since intense straining caused reorientation of the actin cytoskeleton within 90 min in all cell types (Faust *et al.*, 2011), this argues for a strain resilience limit above applied strain parameters even with impaired cell-cell adhesion and disrupted keratin networks in K14R131P cells (Figure 5a'-d'). In agreement, heterozygous expression of human K14R125P in human keratinocytes from a healthy donor exhibited no obvious defects upon large uniaxial strains (Beriault *et al.*, 2012).

K14R131P reduces stiffness of keratinocytes

Recently, AFM and optical stretcher measurements of WT and keratin-free keratinocytes showed that loss of keratins significantly decreased stiffness of keratinocytes (Ramms *et al.*, 2013; Seltmann *et al.*, 2013a). Since the K14R131P mutation prevented keratin network formation, we performed AFM indentation experiments to assess the influence of this EBS-relevant point mutation on mechanical properties of epidermal cells.

Conduction of AFM measurements on single cells revealed that *Ktyl*^{-/-} keratinocytes reached an apparent stiffness (A_2) of 65.1% of the WT level, while re-expression of the single type I keratin K14 restored cellular stiffness to 99.5% (Figure 6a). Plotting the applied forces necessary to reach indentation depths of 100 – 600 nm directly from the raw data confirmed these results, demonstrating that expression of K14 as only type I keratin together with endogenous type II keratins is sufficient to reach a stiffness highly similar to that of the WT level (Figure 6b).

Unexpectedly, the apparent stiffness of K14R131P single cells reached only 51.2% of the WT level and force values necessary to indent for 500 nm and more were significantly lower than those for *Ktyl*^{-/-} cells ($p < 0.05$) (Figure 6a,b,b'). Thus, the point mutation K14R131P changed the stiffness of keratinocytes at the single cell level even more than absence of all keratins. We note that depolymerization of F-actin with latrunculin A, which did not change the difference in cell stiffness between WT and *Ktyl*^{-/-} cells, ruled out a strong influence of actin on mechanical properties (Ramms *et al.*, 2013).

To dissect the respective contribution of desmosomes and keratins to mechanical resilience, we additionally performed AFM indentation cycles on Ca^{2+} -induced cell clusters, more resembling *in vivo* settings. Here, K14 cells reached an apparent stiffness of 64.8% compared to WT levels, while *Ktyl*^{-/-} as well as K14R131P cells were significantly softer and reached 45.6% and 44.9% of WT level, respectively (Figure 6c). Indentation depth experiments revealed significant softening of K14R131P cell clusters compared to K14 and WT controls ($p < 0.001$) (Figure 6d,d'). Unlike in single cells, clusters showed no significant difference between *Ktyl*^{-/-} and K14R131P cells (Figure 6d,d'). AFM

measurements on cell clusters revealed considerable stiffening compared to single cells, reflecting a significant contribution of intercellular junctions to a strain-resilient keratin network in keratinocytes.

Collectively, our data underline the dominant-negative nature of the K14p.Arg125Pro mutation (Coulombe and Lee, 2012; Fuchs and Cleveland, 1998) and suggest that a decrease in cell stiffness and decreased intercellular adhesion contribute to EBS. Cell softness might be a contributor to keratinocyte shape changes observed during tissue repair in an EBS mouse model (Coulombe *et al.*, 1991b). Importantly, K14-positive aggregates in K14R131P cells were insoluble upon Triton X-100 extraction (Figure S2c,d). The exact mechanisms by which mutant keratins ultimately cause cell softening remain to be investigated. Also, a potential impact of keratin mutations on the 3D architecture of the nucleus (Lee *et al.*, 2012) and subsequent changes in gene expression has to be considered.

MATERIALS & METHODS

Cell Culture. Keratinocytes lacking entire type I (KtyI^{-/-}) or type II (KtyII^{-/-}) keratin cluster and WT cells were isolated from respective mice. Mouse lines were generated as described previously for KtyI^{-/-} (Ramms *et al.*, 2013) and KtyII^{-/-} mice (KtyII^{+/-} x mKrt8) (Kroger *et al.*, 2013)(Kumar *et al.*, unpublished). Animal care and experimental procedures were in accordance with the institutional and governmental guidelines.

To generate KtyI^{-/-}K14, KtyI^{-/-}K14R131P, KtyII^{-/-}K5 and KtyII^{-/-}K5E471D cells, mouse K14, K14R131P, K5 or K5E471D cDNAs were cloned into lentiviral pLVX-Puro vector (Clontech). Respective keratin-free keratinocytes stably expressing constructs were generated by lentiviral transduction essentially as described earlier (Seltmann *et al.*, 2013b; Stohr *et al.*, 2012).

Cells were cultured as described previously at 5% CO₂ and 32°C, grown on collagen I- (rat-tail, Invitrogen) coated culture dishes using puromycin (Calbiochem; 8 µg/ml medium) for selection

(Kroger *et al.*, 2013; Ramms *et al.*, 2013). For experiments under high calcium conditions, cells were switched to 1.2mM Ca²⁺ media for 24h.

K14HA construct was subcloned in pcDNA3.1/Zeo vector (Invitrogen) and stably transfected in K14R131P cells followed by subsequent selection with 100 µg/ml zeocin (Invivogen) and 8 µg/ml puromycin. Transient transfections of K14p.Arg131Pro/Cys/His or K5p.Glu471Asp/Gly/Lys in pcDNA3.1/Zeo were performed with Xfect (Clontech) according to manufacturer's protocol.

Immunofluorescence. Fixation of cells with -20°C methanol/acetone and staining was performed as previously described (Kroger *et al.*, 2013). Coverslips were mounted with Prolong Gold (Invitrogen). Immunofluorescence after cell stretch was performed as described previously (Faust *et al.*, 2011). F-actin was visualized with 1% Alexa Fluor 546 or 488 phalloidin (Invitrogen) concurrently to the secondary antibody.

Immunofluorescence microscopy and data processing. Images were recorded with a confocal microscope (LSM 780, Carl Zeiss) or an AxioImager (Carl Zeiss) equipped with 40x or 63x oil immersion objectives and an AxioCam MRm (Carl Zeiss). Image analysis was performed using Zen 2012 Blue software (Carl Zeiss). Images (look up table, brightness and contrast) were adjusted using Photoshop CS4/CS5 (Adobe) and further processed using Illustrator (Adobe) software. Fluorescence micrographs of stretched cells were taken with a confocal microscope (LSM 710, Carl Zeiss), using a 63x/1.4 NA, PH3 oil PlanApochromat objective. The filter sets were appropriate for detection of Alexa Fluor 488 and 564.

Western blotting. SDS-Page and WB was performed as described before (Vijayaraj *et al.*, 2009). For WB of desmosomal proteins, cells were switched to high calcium culture medium 24h prior to cell lysis.

Antibodies. For immunofluorescence and immunoblotting, the following antibodies were used: anti-K14 (rabbit, Magin laboratory); anti-K5 (rabbit, Magin laboratory); anti-K5 head (guinea pig)(Betz *et al.*, 2006); anti-K6 (rabbit, Magin laboratory); anti pan-keratin (rabbit, Progen Biotechnik); anti- α -tubulin (mouse, Sigma-Aldrich); anti-DP 1,2 (mouse, gift from D. Garrod, Manchester, UK); anti-DP 1,2 (guinea pig, Magin laboratory); anti DP-2.17 (mouse, Progen) anti-Dsg 3.10 (mouse, Progen); anti-PKP1 (mouse, Epitomics); anti-HA (mouse; Abcam). Secondary antibodies conjugated to fluorochromes or HRP were purchased from Dianova or Life Technologies.

Dispase Assay. Dispase Assay was performed essentially as described (Hobbs *et al.*, 2011; Kroger *et al.*, 2013).

AFM Measurements. For atomic force microscopy (AFM) analyses on single cells, 60,000 keratinocytes were seeded on collagen I-coated ($6 \mu\text{g}/\text{cm}^2$ collagen, rat-tail, BD Bioscience) cell culture dishes ($\varnothing 35$ mm; VWR) 24h before the experiment. For AFM measurements on confluent cell monolayers, 90,000 keratinocytes were seeded on collagen I-coated cell culture dishes ($\varnothing 35$ mm; VWR) and 24h after plating medium was switched to high calcium for 24h. Immediately before measurements, cells were immersed in freshly prepared HEPES-buffered medium. AFM force spectroscopy on living cells was realized using a Nanowizard Life Science version instrument (JPK) combined with an inverted optical microscope (Axiovert 200, Zeiss) for sample observation. Probing of cell elasticity was performed by using tipless cantilevers ($f_0 = 7$ kHz, $k = 0.04$ N/m; Nanoworld Arrow TL1Au with Ti/ Au back tip coating) equipped with a silica microsphere of a nominal radius of $5 \mu\text{m}$ (G. Kisker GbR, PSI-5.0, surface plain) as described previously (Ramms *et al.*, 2013). For indentation experiments above the nucleus, three force curves were recorded for each position with a cantilever speed of $1.5 \mu\text{m}/\text{s}$ and a force setpoint of 1.5 nN. All indentation measurements were performed above the nucleus.

Force-distance curve analysis. Force-distance curves (F-D curves) were fitted using a standard power law function $F=A\delta^b$, with apparent stiffness A and exponent b as free fit parameters. The general power law function can be regarded as a generalization of the usual Hertz model; for details see (Ramms *et al.*, 2013). Fitting all F-D curves we obtained mean exponent values of 1.96 ± 0.34 (SD). The exponent was therefore fixed to a value of 2 and apparent stiffness (A_2) was fitted for all F-D curves. The parameter-free two-sided Mann-Whitney-Wilcoxon test was used to analyze differences in the distributions of resulting apparent stiffness A_2 .

Cell stretching. Elastomeric chambers of silicone rubber (Sylgard 184, weight ratio 40:1 base to cross-linker) with a flat bottom (20x20 mm) were used for stretching experiments. Manufacturing has been described previously (Faust *et al.*, 2011). After curing for 16h at 60°C, chambers were washed with 2-propanol (Picograde®, LGC Standards GmbH) for 6h and clamped into the stretching device for drying. Pre-stretching prevented sagging of the chamber bottom. Subsequently, chambers were coated with collagen I-solution 6 µg/cm² (rat-tail, BD Bioscience) diluted in 0.02N acetic acid for 30 min at 37°C, rinsed twice with PBS and used for experiments immediately.

150,000 keratinocytes were seeded on stretching chambers 48h before the experiment. 24h after plating, confluent cell layers were switched to high calcium culturing condition. Cell monolayers were either stretched once for 40% or cyclically for 90 min with an amplitude of 14% and a frequency of 4 Hz, at 37°C and 5% CO₂. Cyclic stretching experiments were stopped in stretched position and cells were immediately fixed with 3.7% formalin. 40% stretch experiments were analyzed in phase contrast.

Statistical analysis. Statistical significance was determined by two-tailed t-tests. When equal variance test failed, Wilcoxon-Mann-Whitney Rank Sum test was run (p 0.05=*; p 0.01=**; p 0.005=***).

CONFLICT OF INTEREST

The authors state no conflict of interest.

ACKNOWLEDGEMENT

We thank Stefan Hüttelmaier and Marcell Lederer (Universitätsklinikum Halle, Halle, Germany) for production of lentivirus and transduction of cells. Work in the Magin lab is supported by the Deutsche Forschungsgemeinschaft (MA-1316/9-3, 1316/15-1, 1316/17-1; MA1316/19-1) and the Translational Center for Regenerative Medicine, TRM, Leipzig, PtJ-Bio, 0315883, to T. M. Magin. Work in the Leube lab is supported by the DFG (LE566/-18-1, LE566/20-1) and by the START-Program of the Faculty of Medicine, RWTH Aachen.

Accepted manuscript

FIGURE LEGENDS

Figure 1 | Impact of keratin mutations on cytoskeletal organization. (a) K14 cells assemble into an intact keratin cytoskeleton, while K14R131P cells (a') fail to do so and display aggregates throughout the cytoplasm. (b) Like K5 cells, K5E471D cells (b') form intact keratin filaments. Keratins are visualized by K14 or K5 antibody staining, respectively. (c,d) WB of total protein lysates shows stabilization of the respective endogenous binding partners following re-expression of wildtype (K14, K5) or mutated protein (K14R131P, K5E471D). Bands in (c) and (d) were arranged from the same blot. Scale bars: 10 μ m.

Figure 2 | Impaired desmosome formation in K14R131P but not in K5E471D cells. (a) In K14 cells, desmosomes (visualized by DP staining) form upon Ca^{2+} -induction, along with an intact keratin cytoskeleton (visualized by K14 staining). (a') Presence of impaired desmosomes in K14R131P cells positively correlates with high (H) or low (L) levels of aggregates in individual cells. (a'') Quantification of cell boundary area coverage with desmosomes in dependence of keratin aggregate frequency in K14R131P cells (n=205 (LL); 108 (HH); 210 (HL); for details see Figure S3c-c''). (b,b') In K5 and in K5E471D cells desmosome formation proceeds unimpaired in the presence of intact keratin cytoskeletons. Scale bars: 10 μ m. Error bars are SEM.

Figure 3 | Reduction of desmosomal proteins and impaired epithelial sheet integrity in K14R131P but not in K5E471D cells. (a,a') WB shows reduced amounts of DP in *Ktyl*^{-/-} and K14R131P cells and elevated DP levels upon wildtype K14 re-expression. (b,b') DP levels are restored by re-expression of K5 or K5E471D. Downregulation of DP in *Ktyl*^{-/-} cells was shown in (Kroger *et al.*, 2013). (c) Shear stress assay revealed impaired epithelial sheet integrity in *Ktyl*^{-/-} and in K14R131P mutant cells, while K14 restored WT level. (d) Epithelial sheet integrity remained unaltered by K5E471D compared to K5

expression. Note that reduced epithelial integrity in K5 and K5E471D cells compared to K14 cells correlates with lower level of re-expressed keratins. For each experiment n=3-4; error bars are SEM.

Figure 4 | Implications for EBS therapy approaches. (a,a') Mixing of WT and K14R131P cells in a 1:1 ratio shows formation of cell-cell contacts between WT cells. Defective desmosomes between WT and K14R131P cells suggest trans-dominant effects. (b) Re-expression of K14HA into K14R131P cells shows that attachment of KIF to desmosomes depends on amount of aggregates (compare H and L cells). (c) DP levels are not altered upon re-expression of K14HA in K14R131P cells. (d,d') Re-expression of K14HA in K14R131P cells did not rescue epithelial sheet integrity in the shear stress assay. Scale bars: 10 μ m. For each experiment n=3; error bars are SEM.

Figure 5 | Stretching cells at intermediate amplitudes revealed similar resilience for all cell types. Cells were stretched on elastomeric chambers for 90 min with an amplitude of 14% and a frequency of 4 Hz. Immunofluorescence staining of keratin with pan-keratin antibody for respective cell types is shown in upper panel (a-d). Lower panel (a'-d') displays immunofluorescence for F-actin. Arrowheads indicate direction of applied stretch. Scale bar: 10 μ m

Figure 6 | AFM reveals significant softening of *Ktyl*^{-/-} and K14R131P cells. (a) Apparent stiffness A_2 of single cells obtained from indentation experiments performed above the nucleus of respective cell types (n>32). (b) Plot showing the average forces needed to reach a certain indentation depth in the cell center of single cells (n= 30-38). (b') Significance analysis. Note that K14R131P cells are even softer than *Ktyl*^{-/-} cells. (c) Apparent stiffness A_2 of cell clusters under high Ca^{2+} conditions obtained from indentation experiments above the nucleus (n=43-47). (d) Plot showing the average forces needed to reach a certain indentation depth in a cluster of cells (n=43-47). (d') Significance analysis (*p= 0.05, **p= 0.01, ***p= 0.001); error bars are SD.

REFERENCES

Anton-Lamprecht I, Schnyder UW (1982) Epidermolysis bullosa herpetiformis Dowling-Meara. Report of a case and pathomorphogenesis. *Dermatologica* 164:221-35.

Baek SO, Kim SW, Jung SN, *et al.* (2011) Giant epidermal inclusion facial cyst. *Journal of Craniofacial Surgery* 22:1149-51.

Bar J, Kumar V, Roth W, *et al.* (2014) Skin fragility and impaired desmosomal adhesion in mice lacking all keratins. *Journal of Investigative Dermatology* 134:1012-22.

Beriault DR, Haddad O, McCuaig JV, *et al.* (2012) The mechanical behavior of mutant K14-R125P keratin bundles and networks in NEB-1 keratinocytes. *PLoS One* 7:e31320.

Betz RC, Planko L, Eigelshoven S, *et al.* (2006) Loss-of-function mutations in the keratin 5 gene lead to Dowling-Degos disease. *Am J Hum Genet* 78:510-9.

Cao T, Longley MA, Wang XJ, *et al.* (2001) An inducible mouse model for epidermolysis bullosa simplex: implications for gene therapy. *Journal of Cell Biology* 152:651-6.

Coulombe PA, Hutton ME, Letai A, *et al.* (1991a) Point mutations in human keratin 14 genes of epidermolysis bullosa simplex patients: genetic and functional analyses. *Cell* 66:1301-11.

Coulombe PA, Hutton ME, Vassar R, *et al.* (1991b) A function for keratins and a common thread among different types of epidermolysis bullosa simplex diseases. *Journal of Cell Biology* 115:1661-74.

Coulombe PA, Lee CH (2012) Defining keratin protein function in skin epithelia: epidermolysis bullosa simplex and its aftermath. *Journal of Investigative Dermatology* 132:763-75.

Darwich E, Vicente A, Bolling MC, *et al.* (2011) Extensive acantholysis as the major histological feature of a severe case of Dowling Meara-epidermolysis bullosa simplex: a reappraisal of acantholysis in the newborn. *European Journal of Dermatology* 21:966-71.

Faust U, Hampe N, Rubner W, *et al.* (2011) Cyclic stress at mHz frequencies aligns fibroblasts in direction of zero strain. *PLoS One* 6:e28963.

Fine JD, Bruckner-Tuderman L, Eady RA, *et al.* (2014) Inherited epidermolysis bullosa: updated recommendations on diagnosis and classification. *Journal of the American Academy of Dermatology* 70:1103-26.

Fine JD, Johnson LB, Weiner M, *et al.* (2009) Epidermolysis bullosa and the risk of life-threatening cancers: the National EB Registry experience, 1986-2006. *Journal of the American Academy of Dermatology* 60:203-11.

Fuchs E, Cleveland DW (1998) A structural scaffolding of intermediate filaments in health and disease. *Science* 279:514-9.

Fuchs E, Weber K (1994) Intermediate filaments: structure, dynamics, function, and disease. *Annual Review of Biochemistry* 63:345-82.

Hegde V, Hickerson RP, Nainamalai S, *et al.* (2014) In vivo gene silencing following non-invasive siRNA delivery into the skin using a novel topical formulation. *J Control Release* 196:355-62.

Herrmann H, Wedig T, Porter RM, *et al.* (2002) Characterization of early assembly intermediates of recombinant human keratins. *Journal of Structural Biology* 137:82-96.

Hesse M, Grund C, Herrmann H, *et al.* (2007) A mutation of keratin 18 within the coil 1A consensus motif causes widespread keratin aggregation but cell type-restricted lethality in mice. *Experimental Cell Research* 313:3127-40.

Hobbs RP, Amargo EV, Somasundaram A, *et al.* (2011) The calcium ATPase SERCA2 regulates desmoplakin dynamics and intercellular adhesive strength through modulation of PKC α signaling. *FASEB Journal* 25:990-1001.

Homberg M, Magin TM (2014) Beyond expectations: novel insights into epidermal keratin function and regulation. *Int Rev Cell Mol Biol* 311:265-306.

Intong LR, Murrell DF (2012) Inherited epidermolysis bullosa: new diagnostic criteria and classification. *Clinics in Dermatology* 30:70-7.

Kitajima Y, Inoue S, Yaoita H (1989) Abnormal organization of keratin intermediate filaments in cultured keratinocytes of epidermolysis bullosa simplex. *Archives for Dermatological Research Archiv fur Dermatologische Forschung* 281:5-10.

Kroger C, Loschke F, Schwarz N, *et al.* (2013) Keratins control intercellular adhesion involving PKC-alpha-mediated desmoplakin phosphorylation. *Journal of Cell Biology* 201:681-92.

Lee CH, Kim MS, Chung BM, *et al.* (2012) Structural basis for heteromeric assembly and perinuclear organization of keratin filaments. *Nat Struct Mol Biol* 19:707-15.

Liovic M, D'Alessandro M, Tomic-Canic M, *et al.* (2009) Severe keratin 5 and 14 mutations induce down-regulation of junction proteins in keratinocytes. *Experimental Cell Research* 315:2995-3003.

Liu L, Mellerio JE, Martinez AE, *et al.* (2014) Mutations in EXPH5 result in autosomal recessive inherited skin fragility. *British Journal of Dermatology* 170:196-9.

Ma L, Yamada S, Wirtz D, *et al.* (2001) A 'hot-spot' mutation alters the mechanical properties of keratin filament networks. *Nat Cell Biol* 3:503-6.

Morley SM, D'Alessandro M, Sexton C, *et al.* (2003) Generation and characterization of epidermolysis bullosa simplex cell lines: scratch assays show faster migration with disruptive keratin mutations. *British Journal of Dermatology* 149:46-58.

Ramms L, Fabris G, Windoffer R, *et al.* (2013) Keratins as the main component for the mechanical integrity of keratinocytes. *Proceedings of the National Academy of Sciences of the United States of America* 110:18513-8.

Roth W, Hatzfeld M, Magin TM (2012a) Targeting the palm: a leap forward toward treatment of keratin disorders. *Journal of Investigative Dermatology* 132:1541-2.

Roth W, Kumar V, Beer HD, *et al.* (2012b) Keratin 1 maintains skin integrity and participates in an inflammatory network in skin through interleukin-18. *Journal of Cell Science* 125:5269-79.

Russell D, Andrews PD, James J, *et al.* (2004) Mechanical stress induces profound remodelling of keratin filaments and cell junctions in epidermolysis bullosa simplex keratinocytes. *Journal of Cell Science* 117:5233-43.

Schumann H, Roth W, Has C, *et al.* (2012) Verrucous carcinoma in epidermolysis bullosa simplex is possibly associated with a novel mutation in the keratin 5 gene. *British Journal of Dermatology* 167:929-36.

Seltmann K, Fritsch AW, Kas JA, *et al.* (2013a) Keratins significantly contribute to cell stiffness and impact invasive behavior. *Proceedings of the National Academy of Sciences of the United States of America* 110:18507-12.

Seltmann K, Roth W, Kroger C, *et al.* (2013b) Keratins mediate localization of hemidesmosomes and repress cell motility. *Journal of Investigative Dermatology* 133:181-90.

Simpson CL, Patel DM, Green KJ (2011) Deconstructing the skin: cytoarchitectural determinants of epidermal morphogenesis. *Nat Rev Mol Cell Biol* 12:565-80.

Stacey SN, Sulem P, Masson G, *et al.* (2009) New common variants affecting susceptibility to basal cell carcinoma. *Nature Genetics* 41:909-14.

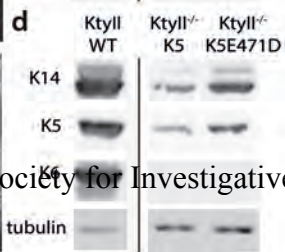
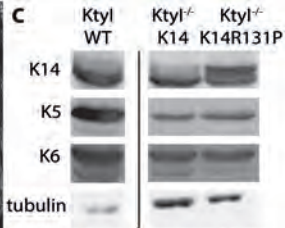
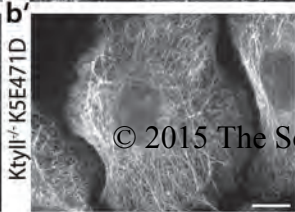
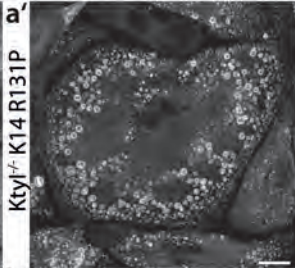
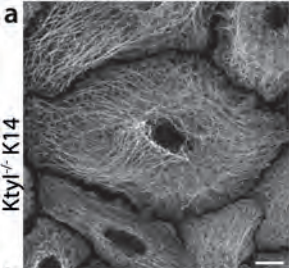
Stohr N, Kohn M, Lederer M, *et al.* (2012) IGF2BP1 promotes cell migration by regulating MK5 and PTEN signaling. *Genes and Development* 26:176-89.

Szeverenyi I, Cassidy AJ, Chung CW, *et al.* (2008) The Human Intermediate Filament Database: comprehensive information on a gene family involved in many human diseases. *Human Mutation* 29:351-60.

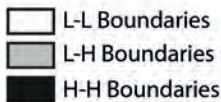
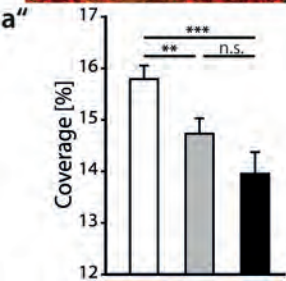
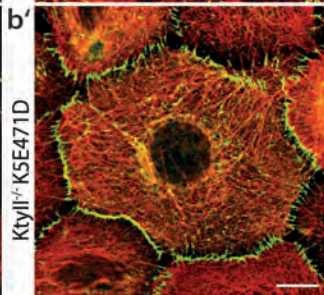
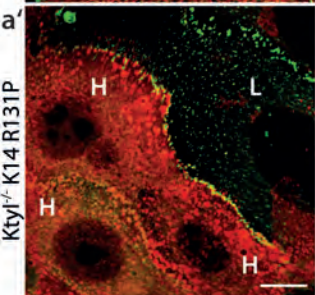
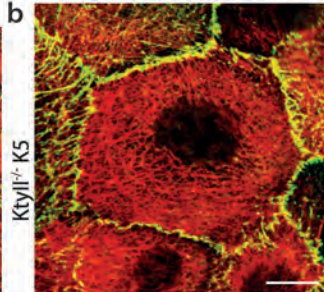
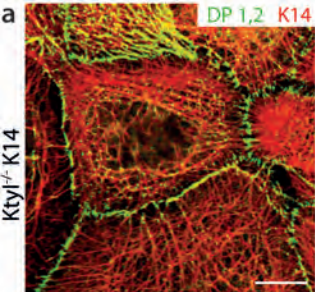
Vijayaraj P, Kroger C, Reuter U, *et al.* (2009) Keratins regulate protein biosynthesis through localization of GLUT1 and -3 upstream of AMP kinase and Raptor. *Journal of Cell Biology* 187:175-84.

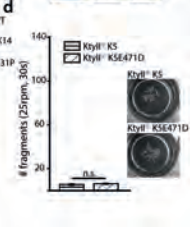
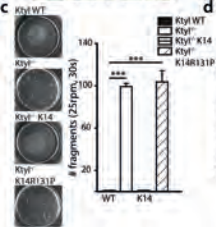
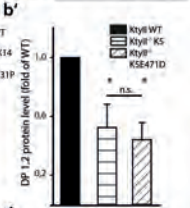
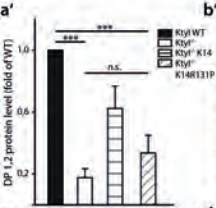
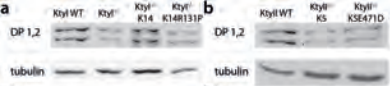
Werner NS, Windoffer R, Strnad P, *et al.* (2004) Epidermolysis bullosa simplex-type mutations alter the dynamics of the keratin cytoskeleton and reveal a contribution of actin to the transport of keratin subunits. *Molecular Biology of the Cell* 15:990-1002.

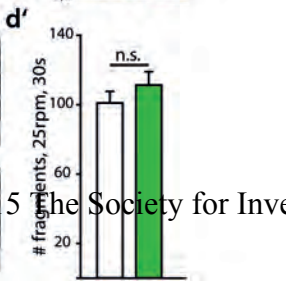
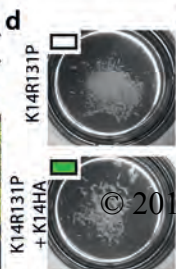
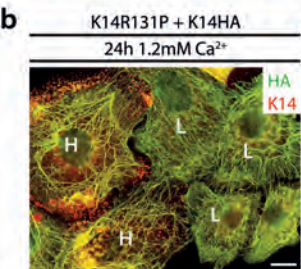
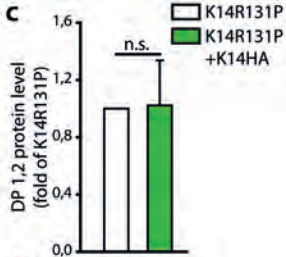
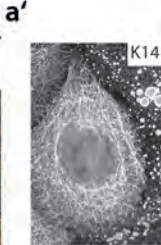
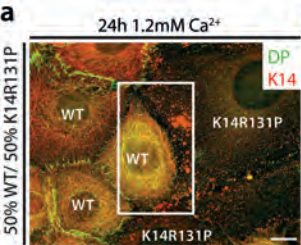
Accepted manuscript

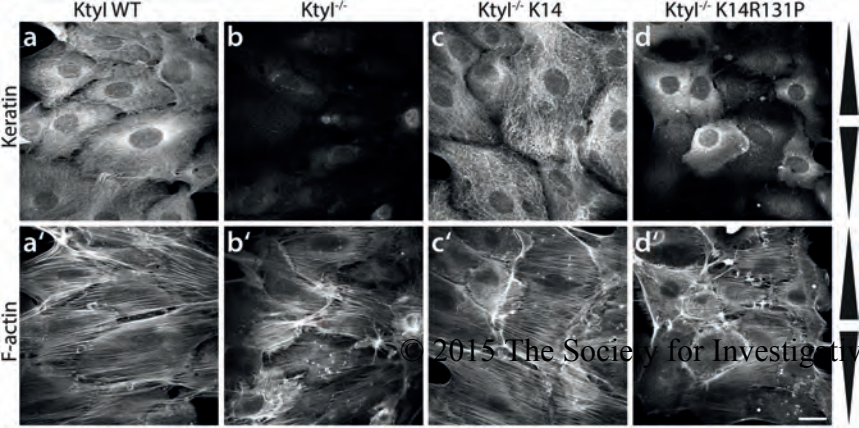


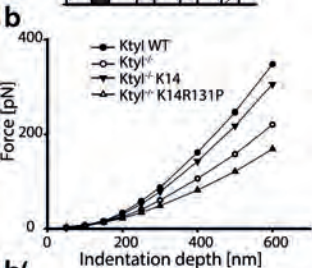
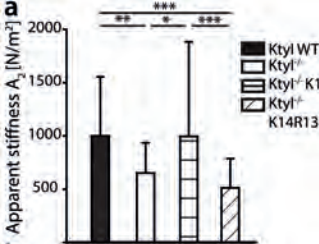
© 2015 The Society for Investigative





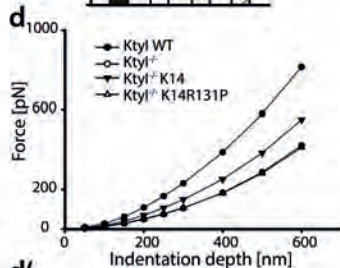
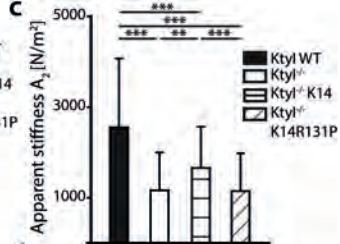






b'

Single cells	300 nm	400 nm	500 nm	600 nm
Ktyl WT				
Ktyl ^{-/-} K14R131P	**	***	***	***
Ktyl ^{-/-}				
Ktyl ^{-/-} K14R131P	-	-	*	+
Ktyl ^{-/-} K14				
Ktyl ^{-/-} K14R131P	*	**	***	***



d'

Cluster	300 nm	400 nm	500 nm	600 nm
Ktyl WT				
Ktyl ^{-/-} K14R131P	***	***	***	***
Ktyl ^{-/-}				
Ktyl ^{-/-} K14R131P				
Ktyl ^{-/-} K14				
Ktyl ^{-/-} K14R131P	**	**	***	**